Journal of the Korean Society of Marine Environment & Safety
Research Paper
Vol. 26, No. 4, pp. 419-428, June 30, 2020, ISSN 1229-3431(Print) / ISSN 2287-3341(Online) https://doi.org/10.7837/kosomes.2020.26.4.419

# The Comparison of Various Turbulence Models of the Flow around a Wall Mounted Square Cylinder

Jun-Young Bae* · Gi-Su Song**†

* Professor, Department of Smart Vehicle, DongJu College, Busan, 49318, Korea
** Senior Engineer, Ship and Offshore Performance Research Center, Samsung Heavy Industries Co. Ltd., Daejeon 34501, Korea

# 벽면에 부착된 사각 실린더 주변 유동에 대한 난류모델 비교연구

배준영* · 송지수**†

* 동주대학교 스마트자동차과 교수, ** 삼성중공업 조선해양연구소 프로

**Abstract :** *The flow past a wall mounted square cylinder, a typical and basic shape of building, bridge or offshore structure, was simulated using URANS computation through adoption of three turbulence models, namely, the k-ε model, k-ω model, and the $v^2$-f model. It is well known that this flow is naturally unstable due to the Karman vortex shedding and exhibits a complex flow structure in the wake region. The mean flow field including velocity profiles and the dominant frequency of flow oscillation that was from the simulations discussed earlier were compared with the experimental data observed by Wang et al. (2004; 2006). Based on these comparisons it was found that the $v^2$-f model is most accurate for the URANS simulation; moreover, the k-ω model is also acceptable. However, the k-ε model was found to be unsuitable in this case. Therefore, $v^2$-f model is proved to be an excellent choice for the analysis of flow with massive separation. Therefore, it is expected to be used in future by studies aiming to control the flow separation.*

**Key Words :** *URANS, Turbulence model, Square cylinder, $v^2$-f model, k-ω model, k-ε model*

**요 약 :** 본 논문에서는 건물, 교량 및 해양구조물에 많이 적용되는 기본적인 형상인 벽면에 부착되어 있는 사각실린더 주변의 유동에 대해, 3개의 난류모델($v^2$-f 모델, k-ω 모델, k-ε 모델)을 적용하여 URANS 수치해석을 각각 수행하고, 그 결과를 비교하였다. 이 유동은 물체의 모서리에서 발생하는 칼만 와(karman vortex) 때문에 본질적으로 강한 비정상성을 가지고 있으며, 물체의 후류 영역에서도 매우 복잡한 유동구조를 가지고 있다고 알려져 있다. 3개의 난류모델이 적용된 수치해석으로부터 예측되는 평균 유동장과 지배적인 유동의 주파수를 Wang et al.(2004; 2006)의 실험결과와 비교하였다. 비교 결과, $v^2$-f 모델이 적용된 URANS 결과가 실험결과와 가장 유사한 결과를 보여주었고, k-ω 모델도 우수한 결과를 보인 반면, k-ε 모델은 본 대상 유동에 적용하기에 부족함을 확인하였다. 따라서 강한 박리가 존재하는 유동의 해석 시에는 $v^2$-f 모델은 좋은 선택이다. 그리고 유동의 박리 제어를 위한 연구에 활용될 것으로 기대된다.

**핵심용어 :** URANS, 난류모델, 사각 실린더, $v^2$-f 모델, k-ω 모델, k-ε 모델

## 1. Introduction

The square cylinder is a typical shape that is applied not only to buildings but also to bridges and off-shore structures. As is well known, however, the separation of the flow in the corner of the square cylinder makes structural vibration. This is fundamentally related to the safety of the structure. Therefore, it is very important to predict the flow field around the square cylinder for the safe design of the various structures. The flow essentially has very complex three-dimensional flow structures and unsteady characteristics. It is difficult to measure precisely flow quantities like velocities and turbulent properties due to complexity of flow in the wake region (Song and He, 1993). Since 1980's, various numerical methodologies such as Large Eddy Simulation (LES) and

* First Author : newthousands@gmail.com, 051-200-1556
† Corresponding Author : kachisu@naver.com, 042-865-4369

Reynolds Averaged Navier-Stokes (RANS) simulations have been adopted to simulate the flow of this kind. Several numerical methods for various flows around a bluff body in a view point of Computational Wind Engineering (CWE) were reviewed (Statopolous, 1997; Murakami, 1998). They discussed the advantages and disadvantages of various methods including limitations and challenges. It is well known that LES produces good results that are closer to experimental data and describes well the unsteady characteristics of the flow. However, computational cost is rather expensive. In contrast, the RANS simulation is much cheaper and practical than LES. Especially, the it could be applied in the flow with high Reynolds number. Indeed, RANS simulation has been still widely used in various real engineering problems.

To solve a turbulent flow in RANS simulation, the turbulence model has to be introduced. After the publication of the standard k-ε model (Launder and Spalding, 1972), various turbulence models have been proposed so far. And some of them have been applied to simulate several practical flows related to CWE. The flow around a wall mounted cube with incoming atmospheric boundary layer was examined by using several versions of k-ε models and LES (Murakami et al., 1996). And investigation of the performance of various turbulence models (RNG k-ε model, low Reynolds number k-ε model, and standard k-ε model) against the flow past a two-dimensional square cylinder was carried out (Lee, 1997). The flow around wall mounted finite square cylinder with the scale ratio 1:2 (width:height) using five different variants of k-ε model were simulated (Mochida et al., 2002).

It was pointed out that Unsteady RANS (URANS) computation provided better accuracy over RANS simulation (Tucker, 2001). This means that unsteady simulation is more appropriate than steady simulation in the fluctuating flow associated with massive separation. The flow past a triangle cylinder using $v^2$-f turbulence model was simulated and the results from RANS and URANS simulations were compared (Durbin, 1995). The mean flow field as well as unsteady features from URANS simulation were much better predicted than those of RANS. The results of RANS and URANS for flows around a square cylinder and over a wall-mounted cube were also compared (Iaccarino et al., 2003). Velocity profiles and the recirculation length behind a square cylinder and wall mounted cube in URANS simulation with $v^2$-f turbulence model agreed much better with the experimental data than those in RANS simulation. It was also concluded that URANS model was sufficient for the prediction of unsteady two-dimensional vortex shedding behind a cylindrical body (Menter et al., 2003). These studies suggest that the URANS simulation can be an efficient approach for computational wind engineering from a practical point of view.

It is well known that the flow around a high-rise building (height/width > 4) has basically unsteady features due to periodic vortex shedding similar to the flow past a square cylinder (Wang et al., 2004; Wang et al., 2006; Sumner et al., 2004; Kawamura et al., 1984). The vibration induced by vortex shedding in cross direction against incoming wind is very important for the structural safety and comfortableness of people who live in a high-rise building. Thus an appropriate turbulence model has to be adopted for realistic computation of a flow field including time-averaged and unsteady features around a high-rise building.

In this study, the flow around wall mounted square cylinder with the scale ratio 1:5 (width:height) is simulated by URANS calculation based on three turbulence models; k-ε model, k-ω model, and $v^2$-f model. The results are compared to experimental data (Wang et al., 2004; Wang et al., 2006). Traditionally several modified models of standard k-ε model have been widely used in CWE despite of some problems such as the “stagnation anomaly” (Strahle, 1985; Durbin, 1996; Durbin and Petterson Reif, 2001). The k-ω model is known to perform better in flows with adverse pressure gradient and has proven to be superior in numerical stability to the k-ε model (Wilcox, 1993; Bardina et al., 1997). As has been stated already, the $v^2$-f model is known to perform very well in URANS simulations of flow past a square cylinder or over a wall mounted cube (Iaccaarino et al., 2003). The aim of the present work is to assess the performance of these three turbulence models in URANS simulation of high-rise building aerodynamics. As the experimental studies (Wang et al., 2004; Wang et al., 2006) reveal most extensively both the steady and unsteady flow field data, we choose this flow as the target flow of the present study.

## 2. Turbulence models

As is well known, the governing equations for the URANS simulation for incompressible flow are as follows.

Continuity equation:

$$\frac{\partial U_i}{\partial x_i} = 0 \tag{1}$$

Momentum equation:

$$\frac{\partial U_i}{\partial t} + U_j \frac{\partial U_i}{\partial x_j} = -\frac{1}{\rho}\frac{\partial P}{\partial x_i} + \frac{\partial}{\partial x_j}\left(2\nu S_{ij} - \tau_{ij}\right) \tag{2}$$

To model the unknown Reynolds stress $\tau_{ij}$, various turbulence models are employed. In this work, we select the following three two-equation based turbulence models. It was pointed out that Unsteady RANS (URANS) computation provided better accuracy over RANS simulation (Tucker, 2001). This means that unsteady simulation is more appropriate than steady simulation in the fluctuating flow associated with massive separation.

### 2.1 k−ε turbulence model

The standard k-ε turbulence model (Launder and Spalding, 1972) and its variants have been widely used. As for bluff body flows, however, the standard k-ε model is known to have a serious drawback. The 'problem of k-ε stagnation point anomaly' which refers to an anomalously large growth of turbulent kinetic energy in stagnation point flows was pointed out (Strahle, 1985). The replacement of rate of strain by vorticity in production term to avoid stagnation point anomaly was suggested (Kato and Launder, 1993). Later it was found that this device causes spurious production in rotating or swirling flow (Durbin, 1996). It was also indicated that the RNG k-ε model and the low Reynolds number k-ε model are found to successfully reproduce the unsteady force coefficients without piling up turbulent kinetic energy near the forward stagnation point, which has been regarded as a fundamental deficiency of the standard k-ε model (Lee, 1997). Despite of this inadequacy, we intentionally adopt a standard form of k-ε model as it is often employed in engineering practice. We adopt the k-ε model (Launder and Sharma, 1974). It is known that this model is numerically more stable than the standard k-ε turbulence model (Bardina et al., 1997). Model equations:

$$\frac{\partial k}{\partial t}+\frac{\partial}{\partial x_j}\left(U_j k-\left(\nu+\frac{\nu_t}{\sigma_k}\right)\frac{\partial k}{\partial x_j}\right)=\mathrm{P}-\varepsilon+\Phi_k \tag{3}$$

$$\frac{\partial \varepsilon}{\partial t}+\frac{\partial}{\partial x_j}\left(U_j \varepsilon-\left(\nu+\frac{\nu_t}{\sigma_\varepsilon}\right)\frac{\partial \varepsilon}{\partial x_j}\right)=c_{\varepsilon 1}\frac{\varepsilon}{k}\mathrm{P}-c_{\varepsilon 2}f_2\frac{\varepsilon^2}{k}+\Phi_\varepsilon \tag{4}$$

P is a production term in eq. (3) and (4). The model constants and various functions in the above equations are given as

$$c_\mu=0.09,\ c_{\varepsilon 1}=1.45,\ c_{\varepsilon 2}=1.92,\ \sigma_{\mathrm{k}}=1.0,\ \sigma_\varepsilon=1.3,$$

$$\nu_t=c_\mu f_\mu\frac{k^2}{\varepsilon},\ \Phi_k=2\nu\left(\frac{\partial\sqrt{k}}{\partial y}\right)^2,\ \Phi_\varepsilon=2\frac{\nu}{\nu_t}\left(\frac{\partial^2 u_s}{\partial y^2}\right)^2$$

$$\mathrm{P}=2\nu_t S_{ij}S_{ij},\quad f_\mu=\exp\left(-3.4/\left(1+0.02\,\mathrm{Re}_t\right)^2\right),$$

$$f_2=1-0.3\exp\left(-\mathrm{Re}_t^2\right),\quad \mathrm{Re}_t=\frac{k^2}{\nu\varepsilon}.$$

Where $\Phi_k$ and $\Phi_\varepsilon$, called by explicit wall term, are added for convenient treatment at the wall, numerically (Jones and Launder, 1972). And $u_s$ is the flow velocity parallel to the wall (Jones and Launder, 1972; Bardina et al., 1997). The boundary conditions at the wall are prescribed as $k=0$, $\varepsilon=0$.

### 2.2 k−ω turbulence model

The two-equation turbulence model using specific rate of dissipation (ω) was proposed (Wilcox, 1993). The wall function at the near wall region is not required in the k-ω model in contrast to the k-ε model where either a wall function approach or low Reynolds number formulation is usually adopted for the near wall treatment (Bardina et al., 1997). It is also known that the k-ω turbulence model is advantageous in simulating unsteady separating flow (Elhadi et al., 2002). Model equations:

$$\frac{\partial k}{\partial t}+\frac{\partial}{\partial x_j}\left(U_j k-\left(\nu+\sigma^*\nu_t\right)\frac{\partial k}{\partial x_j}\right)=\mathrm{P}-\beta^*\omega k \tag{5}$$

$$\frac{\partial \omega}{\partial t}+\frac{\partial}{\partial x_j}\left(U_j \omega-\left(\nu+\sigma\nu_t\right)\frac{\partial \omega}{\partial x_j}\right)=\alpha\frac{\omega}{k}\mathrm{P}-\beta\omega^2 \tag{6}$$

The model constants and the eddy viscosity are given by

$$\alpha=\frac{5}{9},\ \beta=\frac{3}{40},\ \beta^*=\frac{9}{100},\ \sigma^*=0.5,\ \sigma=0.5,\ \text{and}\ \nu_t=\frac{k}{\omega}.$$

Typical boundary conditions at the wall are specified as

$$k=0,\quad \omega=\frac{60\nu}{\beta\left(y_1\right)^2}$$

where $y_1$ is the physical distance of the first grid point away from the wall.

### 2.3 v²−f turbulence model

The $v^2$-f turbulence model was proposed (Durbin, 1995) as a limited form of second moment closure model. Since its introduction, the model is also widely used. It is capable of reproducing the damping of turbulence transport near solid boundaries and the wall non-local effects of pressure deformation fluctuation (Durbin and Petterson Reif, 2001). This model adds two equations of $v^2$ and f to k-ε turbulence model. The quantity $v^2$ is a representative component of the Reynolds stress and f is an elliptic function. Various unsteady flows such as backward facing step flow and flow around a wall mounted cube were examined to

check the capability of $v^2$-f model (Manceau et al., 2000; Iaccarino et al., 2003). Model equations:

$$\frac{\partial k}{\partial t}+\frac{\partial}{\partial x_j}\left(U_j k-\left(\nu+\frac{\nu_t}{\sigma_k}\right)\frac{\partial k}{\partial x_j}\right)=\mathrm{P}-\varepsilon \tag{7}$$

$$\frac{\partial \varepsilon}{\partial t}+\frac{\partial}{\partial x_j}\left(U_j \varepsilon-\left(\nu+\frac{\nu_t}{\sigma_\varepsilon}\right)\frac{\partial \varepsilon}{\partial x_j}\right)=\frac{c_{\varepsilon 1}^{'}\mathrm{P}-c_{\varepsilon 2}\varepsilon}{T} \tag{8}$$

$$\frac{\partial \upsilon^2}{\partial t}+\frac{\partial}{\partial x_j}\left(U_j \upsilon^2-(\nu+\nu_t)\frac{\partial \upsilon^2}{\partial x_j}\right)=kf-\upsilon^2\frac{\varepsilon}{k} \tag{9}$$

$$L^2\nabla f-f=(1-c_1)\frac{\left[\frac{2}{3}-\frac{\upsilon^2}{k}\right]}{T}-c_2\frac{\mathrm{P}}{k} \tag{10}$$

The model constants and several functions in the above equations are:

$$L=C_L l,\ l^2=\max\left[\frac{k^3}{\varepsilon^2},C_\eta^2\left(\frac{\nu^3}{\varepsilon}\right)^{\frac{1}{2}}\right],\ T=\max\left[\frac{k}{\varepsilon},6\left(\frac{\nu}{\varepsilon}\right)^{\frac{1}{2}}\right],$$

$$c_{\varepsilon 1}^{'}=1.4\times\left(1+0.045\left(\frac{k}{\upsilon^2}\right)^{1/2}\right),\ C_\mu=0.22,\ c_1=1.4,$$

$$c_2=0.3,\ c_{\varepsilon 2}=1.9,\ \sigma_\varepsilon=1.3,\ C_L=0.25,\ \mathrm{C}_\eta=85.0,\ \nu_t=C_\mu\upsilon^2 T.$$

In the $v^2$-f turbulence model, boundary conditions at the no-slip surface are usually prescribed as

$$k=0,\ \upsilon^2=0,\ \varepsilon=\frac{2\nu k}{y^2},\ f=-\frac{20\nu^2\upsilon^2}{\varepsilon y^4}$$

Where y is the normal distance from a wall (Manceau et al., 2000; Rahman and Siikonen, 2007).

## 3. Computational detail

The target flow for the present simulation is the flow past a wall mounted square cylinder studied experimentally (Wang et al., 2004; Wang et al., 2006). The computation domain, similar to the experimental arrangement, was selected and the non-dimensional size of computation domain was defined based on the width of the square cylinder, as shown in Fig. 1. The Reynolds number (Red) based on the width of the square cylinder (d) and the free stream velocity (U) is 11,540. Actually, the width of the square cylinder (d) is 2cm in experimental study (Wang et al., 2004; Wang et al., 2006).

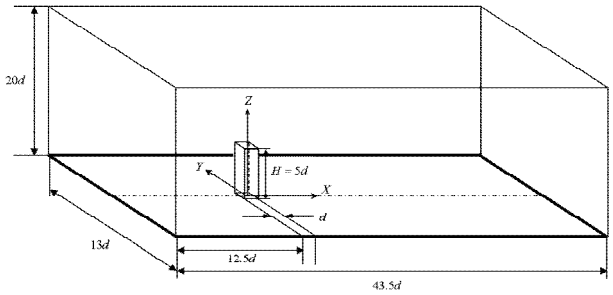


Fig. 1. Computational domain.

Three different types of inflow condition were defined in wind-tunnel tests (Wang et al., 2006) and the flow characteristics behind the building model at each inflow condition were investigated. In the present work, we choose one case of their experiment for simulation in which the free stream turbulence intensity is about 1.2 %. The boundary condition is shown in Fig. 2. Periodic boundary condition was imposed in the spanwise direction. At the upper boundary surface we specified the slip boundary condition ($\frac{\partial U}{\partial z}=0$, $V=0$ and $W=0$). At the outflow boundary we adopted the Neumann boundary conditions for the velocity so that $\frac{\partial U}{\partial x}=\frac{\partial V}{\partial x}=\frac{\partial W}{\partial x}=0$. At all the surface boundaries, no slip condition was imposed.

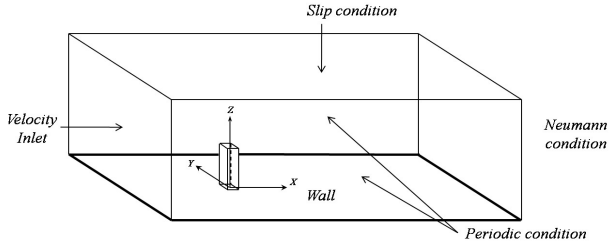


Fig. 2. Boundary condition.

Prior to URANS simulation using three turbulence models, we first carried out a URANS simulation to find out a proper grid system using a k-ω model. Four grid systems as given in Table 1 were tested and designed on the structured grid system. In Fig. 3, the time-averaged streamwise velocity (U) profiles at four downstream positions (x/d=1, 2, 4, and 6, y/d=0) in the wake region were compared. From the velocity profiles of Fig. 3, we find that 'Grid 3' is good enough to generate grid independent solutions. The minimum $\triangle z^+$ at the center of the top surface of the building is 1.71. The number of grids covering the region of the square cylinder is (28, 28, 46) and the shape of 'Grid 3' is presented in Fig. 4.

Table 1. Grid system

| Case | Total number of grids ($N_X$, $N_Y$, $N_Z$) | Number of grids on square cylinder ($N_X$, $N_Y$, $N_Z$) | Minimum grid resolution |
|---|---|---|---|
| Grid 1 | 143,86,86 | 28,28,44 | $\triangle z^+$=3.91 |
| Grid 2 | 171,115,115 | 37,37,58 | $\triangle z^+$=2.12 |
| Grid 3 | 199,137,137 | 45,45,72 | $\triangle z^+$=1.71 |
| Grid 4 | 247,157,157 | 54,54,86 | $\triangle z^+$=1.27 |

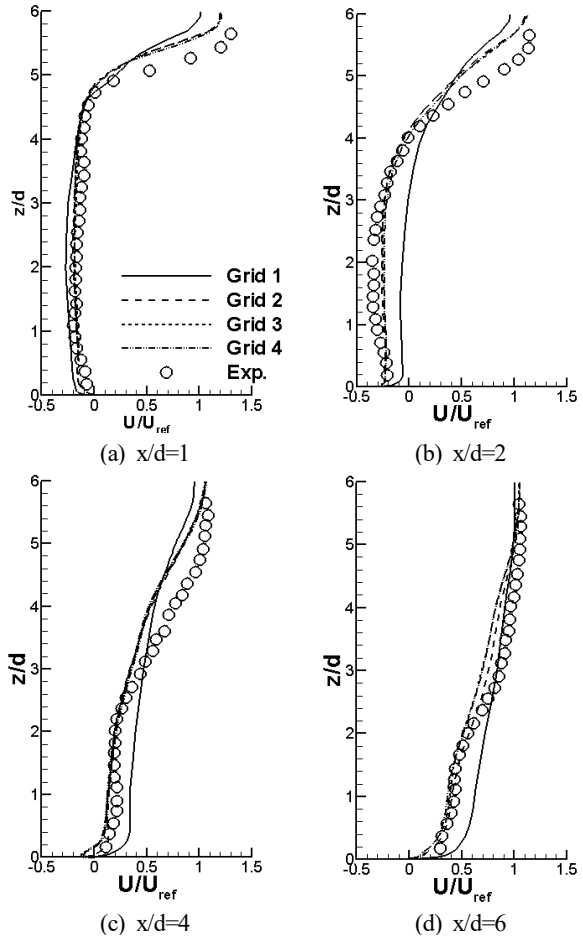


(a) x/d=1 (b) x/d=2

(c) x/d=4 (d) x/d=6

Fig. 3. U velocity profiles at four positions for grid test.

For URANS simulation, we employed an in-house incompressible Navier-Stokes solver (Constantinescu and Squires, 2004; Chang et al., 2007). The three dimensional incompressible Navier-Stokes equations with non-dimensional variables such as length, velocity and density are integrated using a fully implicit fractional step method. The governing equations are transformed to generalized curvilinear coordinates on a non-staggered grid. The convection term is discretized using a 5th order upwind scheme and all the other terms in momentum and pressure-Poisson equation are approximated using the second-order central difference scheme. Time integration is done using dual-time-stepping algorithm and local time stepping method (Constantinescu and Squires, 2004).

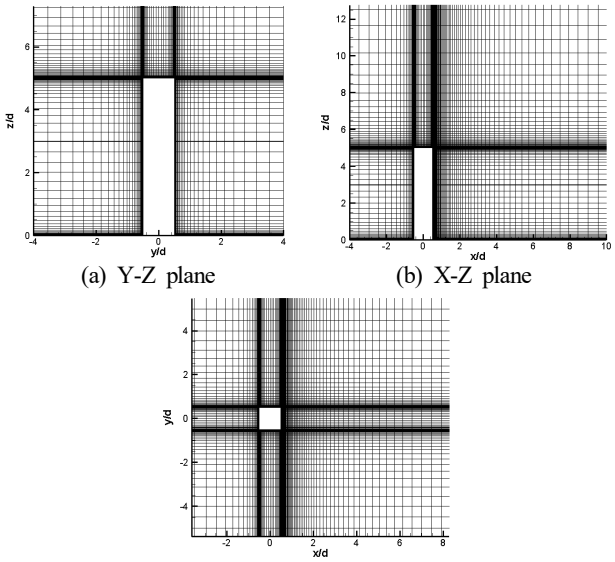


(a) Y-Z plane (b) X-Z plane

(c) X-Y plane

Fig. 4. Grid system.

## 4. Results

As already mentioned, one of the characteristics of the present flow is a periodic vortex shedding. For the simulated flow field to exhibit periodical vortex shedding, a transient computational time period has to be passed from the start of the calculation with initial data. To define mean flow field of URANS simulation, the flow data during this transient time period should be excluded from the averaging process. In the present case, the mean flow field variables were obtained by time-averaging over 150 non-dimensional time after the transient period. This time period amounts to about 15 ~ 16 vortex shedding cycles.

The streamwise velocity (U) profiles at 4 streamwise stations (x/d=1, 2, 4, and 6; y/d=0) are compared in Fig. 5. In the near wake region (x/d < 2), the velocity profiles from the three turbulence models are similar each other except for the region above the square cylinder (z/d > 5). However, the difference among the velocity profiles becomes greater at further downstream stations. The velocity profiles obtained by using the $v^2$-f model are seen to agree best with the experimental data at x/d=4 and 6. The recirculation length estimated from the velocity profiles shown in Fig. 5 from the k-ε model is found to be much greater than those

of the experimental data and the two other turbulence model cases. The vertical velocity (W) profiles at the center plane (y/d=0) are given in Fig. 6. We again see that the velocity profile by using the k-ε model exhibits largest discrepancy from the experimental data and the k-ω model, $v^2$-f model perform similarly.

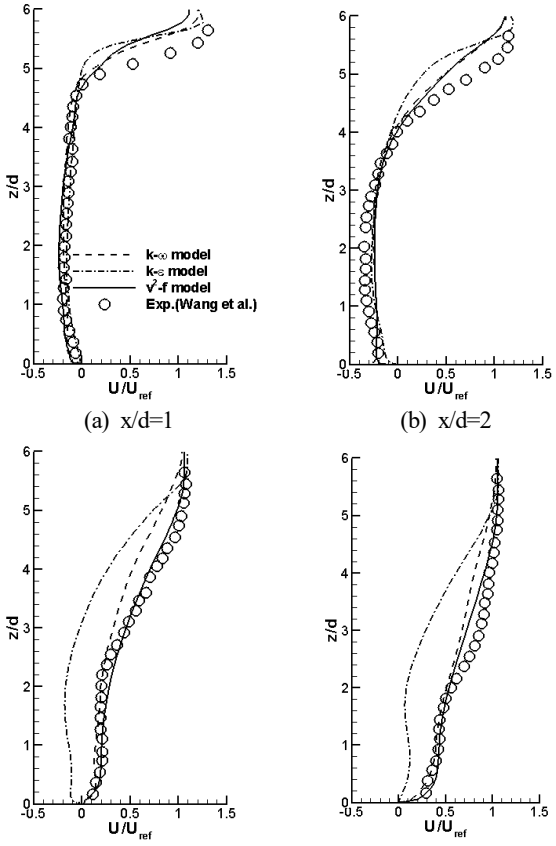


(a) x/d=1 (b) x/d=2

(c) x/d=4 (d) x/d=6

Fig. 5. U velocity profile comparison at four downstream stations.

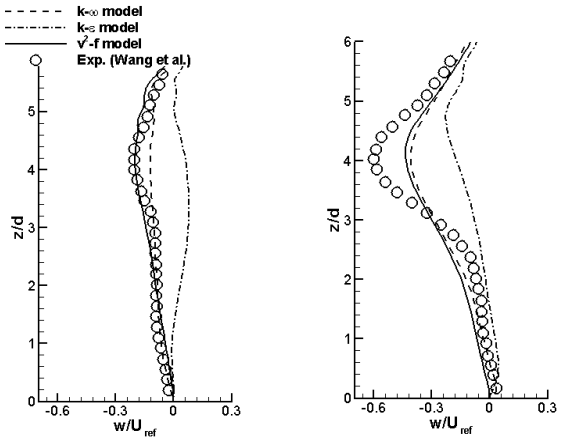


(a) x/d=1 (b) x/d=2

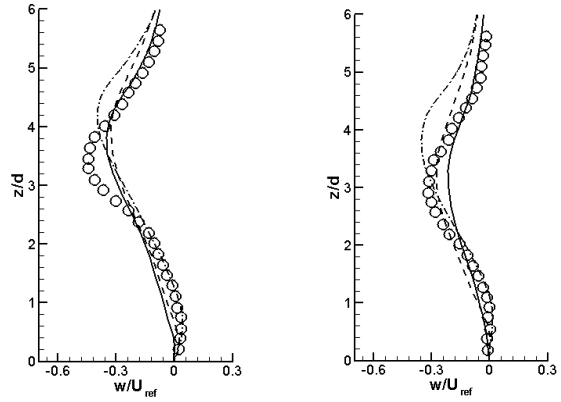


(c) x/d=4 (d) x/d=6

Fig. 6. W velocity profile comparison at four downstream stations.

Fig. 7 illustrates the time averaged streamlines at the center plane (y/d=0). We easily see that the streamline pattern from the $v^2$-f model prediction agrees best to that of the experimental data. The k-ω model predicted pattern looks much closer to the experimental pattern as in the case of $v^2$-f model than the k-ε model case. We note that the saddle point region in the streamline pattern of the $v^2$-f model case is in better agreement with the experimental data than the k-ω model case. Based on the Fig. 7, the saddle point (at y/d=0 plane) was compared in Table 2.

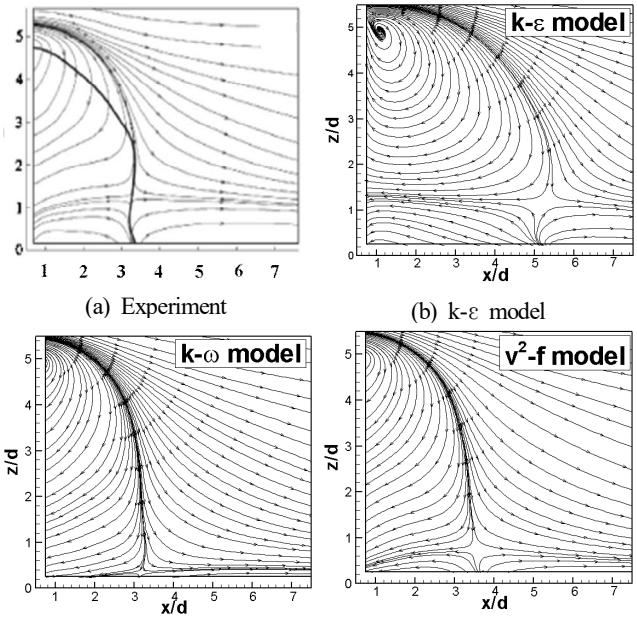


(a) Experiment (b) k-ε model

(c) k-ω model (d) $v^2$-f model

Fig. 7. Time averaged streamlines at center plane.

Table 2. The comparison of the saddle point

| | Exp. [28] | k-ε model | k-ω model | $v^2$-f model |
|---|---|---|---|---|
| x/d | About 3.4 | 5.3 | 3.2 | 3.5 |
| z/d | About 1.3 | 1.2 | 0.3 | 0.7 |

In Fig. 8, the time averaged U velocity contours at the center plane (y/d=0) and X-Y plane (z/d=3.0) are presented. Like to the Fig. 7, the recirculation region from k-ε model is larger than other two model's simulation result. The contour from the $v^2$-f model simulation is overall similar to that from k-ω model.

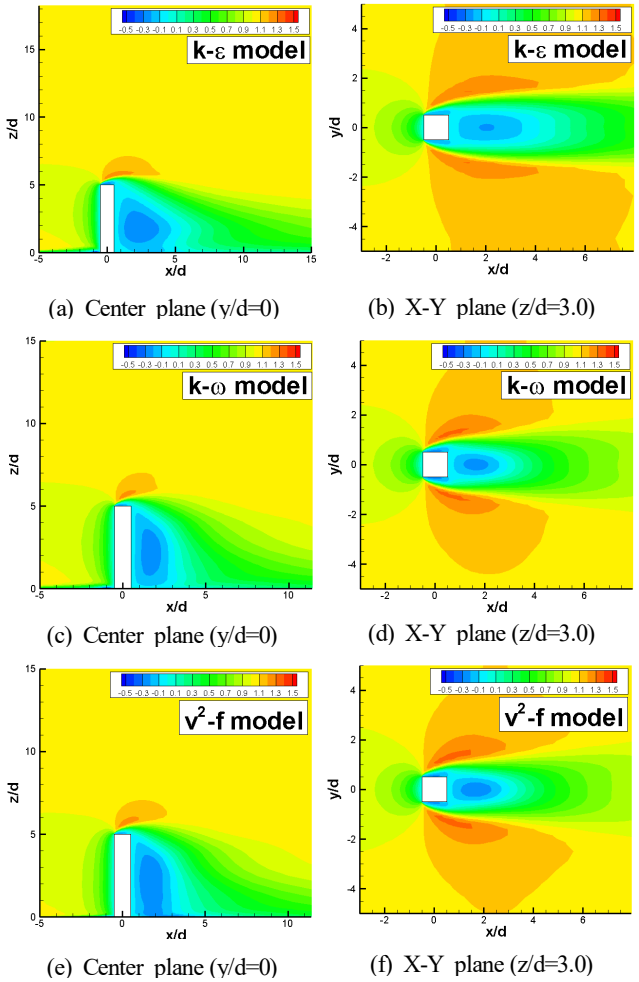


(a) Center plane (y/d=0) (b) X-Y plane (z/d=3.0)

(c) Center plane (y/d=0) (d) X-Y plane (z/d=3.0)

(e) Center plane (y/d=0) (f) X-Y plane (z/d=3.0)

Fig. 8 Time averaged U velocity contours at different two planes.

The spanwise distributions of streamwise velocity (U) and spanwise velocity (V) at several heights (z/d=1, 2.5, and 4) are presented in Figs. 9 and 10, respectively. Both figures clearly demonstrate that the k-ε model performs poorly. While the k-ω model and the $v^2$-f model produce similar profiles; a careful scrutiny of the profiles given in Figs. 9 and 10 leads us to realize that the $v^2$-f model performs slightly better than the k-ω model.

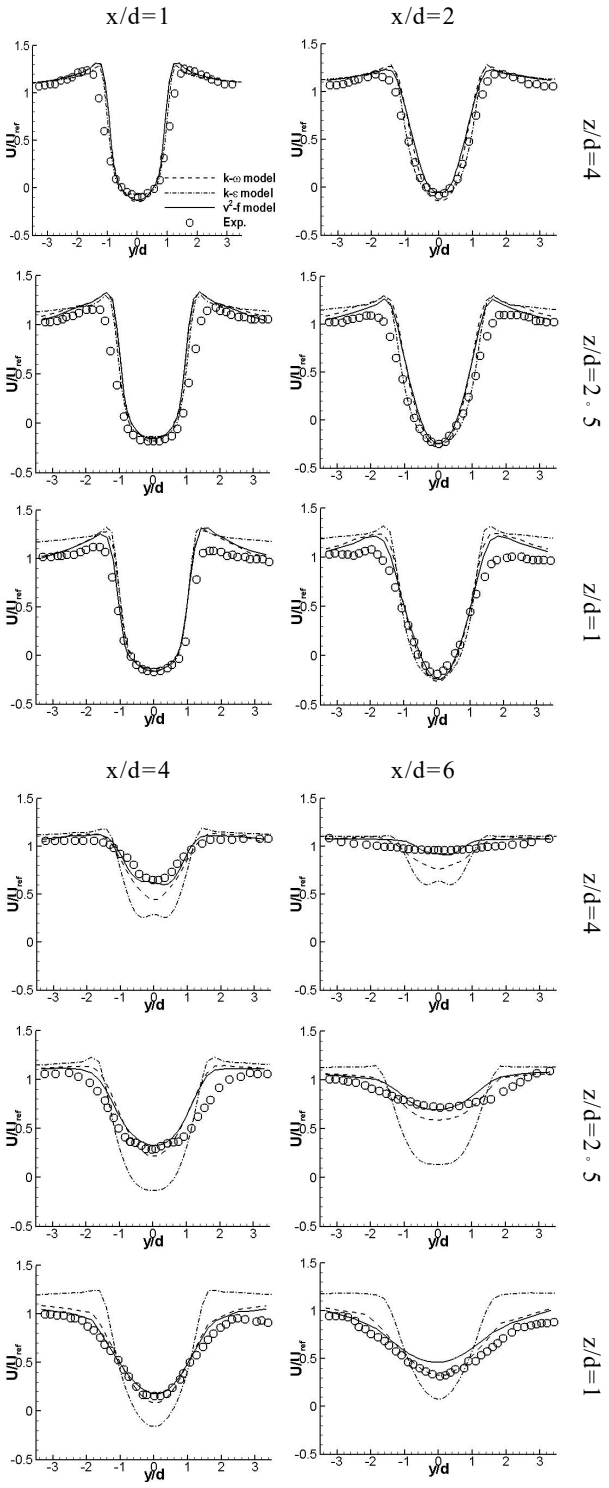


Fig. 9. Spanwise distributions of U velocity at various heights.

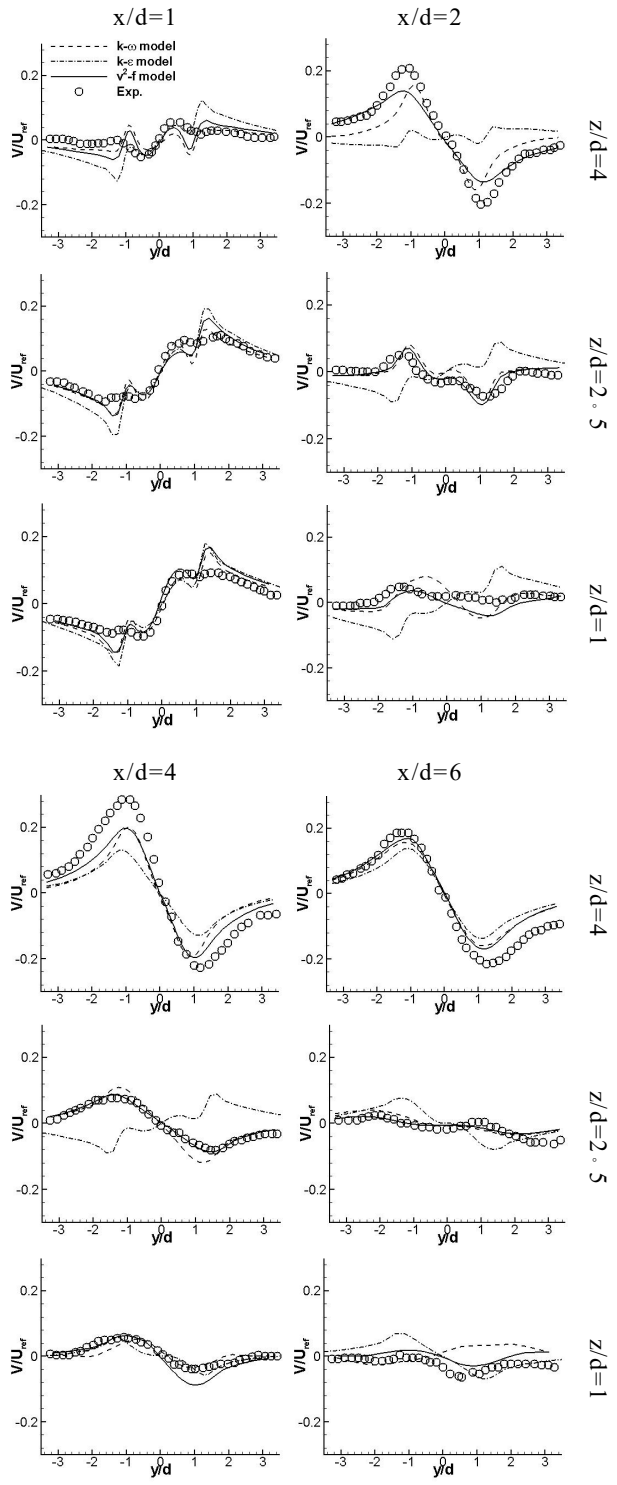


Fig. 10. Spanwise distributions of V velocity at various heights.

The flow past a wall mounted cylinder is naturally unstable due to a large scale flow separation. The dominant mechanism of the flow unsteadiness is the well known Karman vortex shedding as pointed out by many investigators. It is also reported that the oscillating flow pattern at the half height plane of a long wall mounted square cylinder is very similar to that of the flow around a two-dimensional square cylinder (Song and He, 1993; Wang et al., 2004).

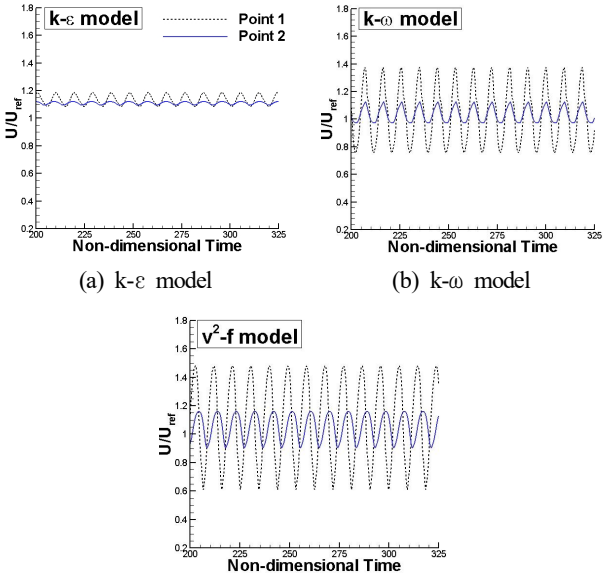


(a) k-ε model (b) k-ω model

(c) $v^2$-f model

Fig. 11. Time histories of U velocity at two positions.

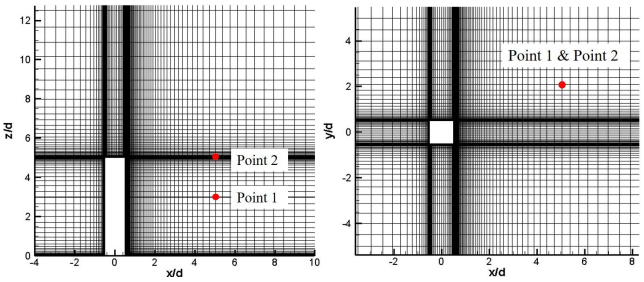


(a) X-Z plane (b) X-Y plane

Fig. 12. The location of two points.

To examine the predictability of the flow unsteadiness, we present in Fig. 11 the time history of streamwise velocity at two different locations: one point (point 1) at the mid height of the cylinder (x/d=5, z/d=3, and y/d=2) and the other (point 2) at the free end of the cylinder (x/d=5, z/d=5, and y/d=2). The location of point 1 and point 2 is presented in Fig. 12.

These positions correspond to those of the measurement positions (Wang et al., 2004). Fig. 11 indicates clearly that the amplitudes of velocity oscillation depend strongly on the turbulence

models employed. We also see that the amplitude of fluctuation monitored at the point of mid-height is much greater than that at the point of free end of the cylinder as expected. The same tendency was observed in flow past a wall mounted circular cylinder (Sumner et al., 2004; Okamoto and Yagita, 1973). Strouhal numbers obtained by FFT from streamwise velocity (U) histories on the two points in the present simulations are illustrated with experimental data in Fig. 13.

The dominant Strouhal numbers are summarized in Table 3.

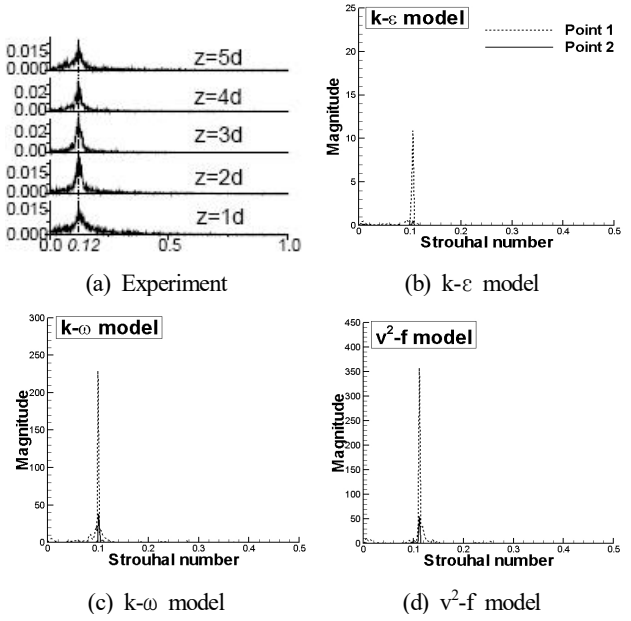


(a) Experiment (b) k-ε model

(c) k-ω model (d) $v^2$-f model

Fig. 13. Dominant frequency of U velocity at two positions.

Table 3. Dominant frequency at two positions

| Simulations and experiments | Strouhal number (=fd/$U_\infty$) |
|---|---|
| k-ε model | 0.104 |
| k-ω model | 0.101 |
| $v^2$-f model | 0.110 |
| Exp. (Wang et al., 2004) | 0.120 |

In the experiment (Wang et al., 2004), the Strouhal number of the dominant peak was 0.12. From Table 3, we confirm that the Strouhal number in $v^2$-f model is the closest to the experimental data. As illustrated in Fig. 13, the dominant frequency measured in experiment (Wang et al., 2004) remained almost the same at various height. This tendency was also observed in a wall mounted finite circular cylinder (Sumner et al., 2004). The present simulation results monitored at two different heights show the same trend.

## 5. Conclusion

In this study, URANS simulations using three different turbulence models (k-ε model, k-ω model, and $v^2$-f model) were carried out for the flow past a wall mounted square cylinder of the scale ratio 1:5 (width:height). The results of the simulation are compared with the experimental data (Wang et al., 2004; Wang et al., 2006).

Based on these simulations,

(1) The $v^2$-f model showed the best performance comparing to the other two-equation turbulence models. Time averaged quantities such as U velocity and V velocity profiles, Streamline are similar to those of experimental study.

(2) Unsteady quantity such as vortex shedding frequency fundamentally induced by flow separation at the corner of square cylinder is also predicted well comparing to that of experimental study.

(3) The $v^2$-f model can be the considerable option for URANS simulation in flow with massive separation.

(4) Even though the scale ratio (width:height) of square cylinder is increased, it is inferred that there is no significant difference which is evaluated by three turbulence models, we examined.

In addition, it is expected that the $v^2$-f model would be applicable in research on control of vortex shedding frequency or design for geometry to reduce the strength of flow separation.

## References

[1] Bardina, J. E., P. G. Huang, and T. J. Coakley(1997), Turbulence modeling validation, testing, and development, NASA TM-110446.

[2] Chang, K. S., G. Constantinescu, and S. O. Park(2007), Assessment of predictive capabilities of detached eddy simulation to simulate flow and mass transport past open cavities, J. Fluids Eng., Vol. 129, pp. 1372-1383.

[3] Constantinescu, G. and K. Squires(2004), Numerical investigations of flow over a sphere in the subcritical and supercritical regimes, Phys. Fluids., Vol. 16, No. 5, pp. 1449-1466.

[4] Durbin, P. A.(1995), Separated flow computations with the k-ε-$v^2$ model, AIAA J., Vol. 33, No. 4, pp. 659-664.

[5] Durbin, P. A.(1996), On the k-ε stagnation point anomaly,

Int. J. Heat & Fluid F., Vol. 17, pp. 89-90.

[6] Durbin, P. A. and B. A. Petterson Reif(2001), Statistical theory and modeling for turbulent flows. John Wiley & Sons, New York, NY 10158-0012, USA.

[7] Elhadi, E. E., X. Lei, and K. Wu(2002), Numerical simulation of 2D separated flow using two different turbulence models, Pakistan Jou. Sci. Pub., Vol. 2, No. 12, pp. 1057-1062.

[8] Iaccarino, G., A. Ooi, P. A. Durbin, and M. Behnia(2003), Reynolds averaged simulation of unsteady separated flow, Int. J. Heat & Fluid F., Vol. 24, pp. 174-156.

[9] Jones, W. P. and B. E. Launder(1972), The prediction of laminarization with a two-equation model of turbulence, Int. J. Heat Transfer, Vol. 15, pp. 301-314.

[10] Kawamura, T., M. Hiwada, T. Hibino, I. Mabuch, and M. Kumada(1984), Flow around a finite circular cylinder on a flat plate, Bull. of JSME., Vol. 27, pp. 2142-2151.

[11] Kato, M. and B. E. Launder(1993), The modeling of turbulent flow around stationary and vibrating square cylinders, In 9th Symp. on Turbulent Shear Flows, Kyoto, Japan, Aug.

[12] Launder, B. E. and B. I. Sharma(1974), Application of the energy dissipation model of turbulence to the calculation of flow near a spinning disc, Lett. Heat & Mass T., Vol. 1, No. 2, pp. 131-138.

[13] Launder, B. E. and J. L. Spalding(1972), Mathematical models of turbulence, Academic Press, New York, USA.

[14] Lee, S. S.(1997), Unsteady aerodynamics force prediction on a square cylinder using k-ε turbulence model, J. Wind Eng. Ind. Aerodyn., Vol. 67&68, pp. 79-90.

[15] Manceau, R., S. Parneix, and D. Laurence(2000), Turbulent heat transfer predictions using the $v^2$-f model on unstructured meshes, Int. J. Heat & Fluid F., Vol. 21, pp. 320-328.

[16] Menter, F. R., M. Kuntz, and R. Bender(2003), A scale-adaptive simulation model for turbulent flow predictions, AIAA paper 2003-0767.

[17] Mochida A., Y. Tominaga S., Murakami, R. Yoshie, T. Ishihara, and R. Ooka(2002), Comparison of various k-e models and DSM applied to flow around a high-rise building - report on AIJ cooperative project for CFD prediction of wind environment, Wind Struct., Vol. 5, No. 2, pp. 227-244.

[18] Murakami, S.(1998), Overview of turbulence models applied in CWE-1997, *J.* Wind Eng. Ind. Aerodyn., Vol. 74&76, pp. 1-24.

[19] Murakami, S., A. Mochida, R. Ooka, S. Kato, and S. Iizuka (1996), Numerical Prediction of Flow around Building with Various Turbulence Models: Comparison of k-ε EVM, ASM, DSM and LES with Wind Tunnel Tests, ASHRAE Trans., Vol. 102, pp. 741-753.

[20] Okamoto, T. and M. Yagita(1973), The experimental investigation on the flow past a circular cylinder of finite length placed normal to the plane surface in a uniform stream, Bull. JSME., Vol. 16, pp. 805-814.

[21] Rahman, M. M. and T. Siikonen(2007), A simplified $v^2$-f model for near-wall turbulence, Int. J. Numer. Meth. Fluids., Vol. 54, pp. 1387-1406.

[22] Song, C. C. S. and J. He(1993), Computation of wind flow around a tall building and the large scale vortex structure, J. Wind Eng. Ind. Aerodyn., Vol. 46&47, pp. 219-228.

[23] Stathopoulos, T.(1997), Computational wind engineering: Past achievements and future challenges, J. Wind Eng. Ind. Aerodyn., Vol. 67&68, pp. 509-532.

[24] Strahle, W. C.(1985), Stagnation point flows with freestream turbulence-the matching condition, AIAA J., Vol. 23, No. 11, pp. 1822-1824.

[25] Sumner, D., J. L. Heseltine, and O. J. P. Dansereau(2004), Vortex shedding from a finite circular cylinder of small aspect ratio, Proceedings of the Canadian Society for Mechanical Engineering Forum 2004 - CSME Forum 2004, London, Canada, June.

[26] Tucker, P. G.(2001), Computation of unsteady internal flows: Fundamental methods with case studies, Kluwer Academic Publishers, Norwell, Massachusetts, USA.

[27] Wang, H. F., Y. Zhou, C. K. Chan, and K. S. Lam(2006), Effect of Initial Conditions on Interaction between a Boundary Layer and a Wall-Mounted Finite-Length-Cylinder Wake, Phys. Fluids., Vol. 18, No. 6, pp. 1-12.

[28] Wang, H. F., Y. Zhou, C. K. Chan, W. O. Wong, and K. S. Lam(2004), Flow Structure around a Finite-Length Square Prism, Proceedings of the 15th Australasian Fluid Mechanics Conference, Sydney, Australia, Dec.

[29] Wilcox, D. C.(1993), Turbulence modeling for CFD, DCW Industries, Inc., 5354 Palm Drive, La Canada, Calif., USA.

Received : 2020. 04. 20.
Revised : 2020. 05. 29. (1st)
: 2020. 06. 05. (2nd)
Accepted : 2020. 06. 26.